Available online at www.sciencedirect.com
ScienceDirect
Journal of the European Ceramic Society 30 (2010) 899–904
www.elsevier.com/locate/jeurceramsoc

Manipulating microstructure and mechanical properties of CuO doped 3Y-TZP nano-ceramics using spark-plasma sintering

Shen Ran [a], Jozef Vleugels [c], Shuigen Huang [c], Kim Vanmeensel [c], Dave H.A. Blank [a], Louis Winnubst [b,*]

[a] *Inorganic Materials Science, MESA+ Institute for Nanotechnology, University of Twente, P.O. Box 217, 7500 AE Enschede, The Netherlands*
[b] *Inorganic Membranes, Membrane Technology Group, MESA+ Institute for Nanotechnology, University of Twente, P.O. Box 217, 7500 AE Enschede, The Netherlands*
[c] *Department of Metallurgy and Materials Engineering (MTM), K.U. Leuven, Kasteelpark Arenberg 44, B-3001 Leuven, Belgium*

Received 29 June 2009; received in revised form 28 September 2009; accepted 1 October 2009
Available online 5 November 2009

Abstract

Nano-powder composites of 3Y-TZP doped with 8 mol% CuO were processed by spark-plasma sintering (SPS). A 96% dense composite ceramic with an average grain size of 70 nm was obtained by applying the SPS process at 1100 °C and 100 MPa for 1 min. In contrast to normal, pressureless, sintering during SPS reactions between CuO and 3Y-TZP were suppressed, the CuO phase was reduced to metallic Cu, while the 3Y-TZP phase remained almost purely tetragonal. Annealing after SPS results in grain growth and tetragonal to monoclinic zirconia phase transformation. The grain size and monoclinic zirconia phase content are strongly dependent on the annealing temperature. By combining the processing techniques studied in this work, including traditional pressureless sintering, properties of the composite ceramic can be tuned via manipulation of microstructure. Tuning the mechanical properties of dense 8 mol% CuO doped 3Y-TZP composite ceramic by utilising different processing techniques is given as an example.

Keywords: Spark-plasma sintering; Mechanical properties; Microstructure; Zirconia; Copper oxide

1. Introduction

CuO doped 3Y-TZP (3 mol% yttria stabilised tetragonal zirconia polycrystals) composite ceramics have shown special properties including large superplasticity[1,2] and low friction under dry sliding conditions,[3,4] which make this group of material interesting for applications like near net shape forming of ceramics and moving parts to operate under unlubricated conditions. Mechanical properties such as hardness, strength and toughness are also important for potential applications. The superplasticity, tribological properties as well as mechanical properties are highly dependent on microstructure of the materials. A tool of extensive manipulation of microstructure will enable us to obtain suitable materials for different applications.

Recently it has been shown that several reactions occur during sintering of CuO doped 3Y-TZP systems, and that these reactions strongly influence sintering behaviour and microstructure evolution.[5–7] In nanosized CuO doped 3Y-TZP dissolution of CuO in the 3Y-TZP matrix, starting below 600 °C, enhances grain boundary diffusivity and subsequently leads to fast densification in the intermediate sintering stage. At 860 °C a solid-state reaction between CuO and yttria, as segregated to the 3Y-TZP grain boundaries, occurs forming a solid $Y_2Cu_2O_5$ phase which retards densification and induces the formation of the thermodynamic stable monoclinic zirconia phase.[6] Obviously, in order to obtain a CuO doped 3Y-TZP ceramic with the desired microstructure and properties, a good control of all these reactions during sintering is necessary.

In this paper we report that the microstructure (grain size and phase composition) of CuO doped 3Y-TZP nano-ceramics can successfully be manipulated by means of utilising different processing techniques, including pressureless sintering (PLS) and spark-plasma sintering (SPS). The possibility of tuning material

* Corresponding author. Tel.: +31 53 489 2994; fax: +31 53 489 4611.
E-mail address: a.j.a.winnubst@utwente.nl (L. Winnubst).

0955-2219/$ – see front matter © 2009 Elsevier Ltd. All rights reserved.
doi:10.1016/j.jeurceramsoc.2009.10.002

properties by microstructure control is presented via an example of adjusting mechanical properties of the 8 mol% CuO doped 3Y-TZP ceramic.

Spark-plasma sintering (SPS) is a recently developed processing technique, also known as pulsed electric current sintering (PECS) or field assisted sintering (FAST).[8–10] Instead of using an external heating source, SPS employs a pulsed DC current passing through the electrically conducting pressure die and, in appropriate cases, also through the sample. This implies that the die itself acts as a heating source and that the sample is heated from both outside and inside.[9,10] The SPS technique provides several engineering advantages, including very fast heating rate, short processing time and no need for additives or pre-compaction.[9] These advantages give more possibilities to control the microstructure evolution during the ceramic fabrication process and in this way the mechanical, electronic or optical properties of the materials can be adjusted.[10–13]

2. Experimental

Nanocrystalline 3Y-TZP and CuO powders with BET equivalent particle sizes of 10 and 50 nm respectively were prepared by means of co-precipitation and oxalate precipitation, respectively.[5,6,14] Composites of 3Y-TZP doped with 8 mol% of CuO (sample code 3YZ-8C) were prepared by ball-milling followed by subsequent ultrasonic vibration of the milled suspension and drying. For pressureless sintering the composite powder was isostatically pressed into a cylindrical green compact at 400 MPa and a Netzsch 402E dilatometer was used to study sintering behaviour in an oxygen flow as further described in Refs.[5,6] SPS experiments were performed on a FCT FAST device (Type HP D 25/1, FCT Systeme, Rauenstein, Germany). The SPS procedure contains the following segments.

(I) At a pressure of 16 MPa (a load of 5 kN), a constant DC current was applied until the central pyrometer reached its onset temperature (450 °C); (II) after a dwell at 450 °C for 1 min, the temperature was linearly increased to 850 °C at a heating rate of 400 °C min^{-1}; (III) a hold at 850 °C for 1 min while the pressure was increased linearly to 100 MPa; (IV) heating to 1100 °C; (V) dwell at 1100 °C for 1 min; (VI) unloading the pressure and current and free cooling to room temperature. Details on the graphite die/punch set-up and temperature control are provided elsewhere.[9] During SPS processing, the piston movement was recorded as a function of time. This movement relative to the piston position at the start of the process represents the linear axial shrinkage (ΔL), and therefore is a measure for the densification behaviour of the specimen. After the SPS process, all specimens were polished with fine sandpaper to remove the outmost layer, which is contaminated with carbon.

The density was measured according the Archimedes method in mercury. Microstructure of the materials was investigated by scanning electron microscopy (SEM, Thermo NORAN Instruments) and transmission electron microscopy (TEM, CM30 Twin/STEM, Philips). X-ray diffraction (X'pert_APD, PANalytical, using Cu-$K_{\alpha 1}$, $\lambda = 1.542$ Å) was performed for phase analysis. The volume fraction of monoclinic zirconia phase is determined by Toraya's method.[15]

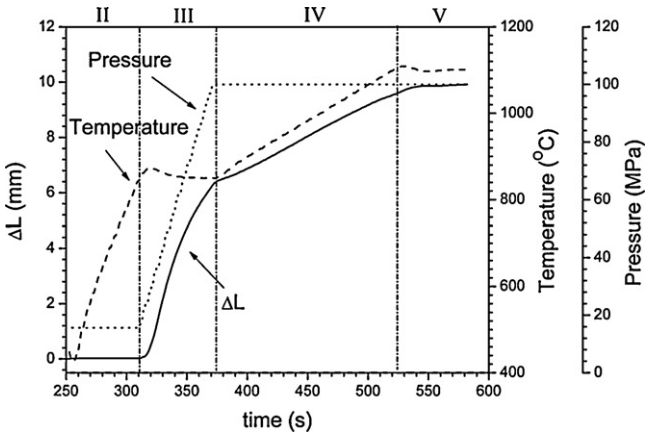

Fig. 1. Densification behaviour of 3TZ-8C nano-powder composite. Piston position at the start of segment II is set as starting point for piston movement distance calculation. Details on the meaning of the several segments are given in Section 2.

The influence of annealing on grain size and zirconia crystal structure was performed on the spark-plasma sintered samples. Here samples were cut and polished with diamond paste (3 μm grade) and annealed at 850, 900, 950, and 1000 °C, respectively, in an oxygen flow for 1 h with a heating and a cooling rate of 15 °C min^{-1} and 2 °C min^{-1}, respectively. The annealed cuts were then analysed by XRD and SEM. Average grain size was determined by using the Mendelson's linear intercept technique.[16]

Vickers hardness and fracture toughness were determined by means of indentation test (Indentation hardness tester, Model FV-700, Future-Tech Corp., Tokyo, Japan). The Vickers hardness, H_V, was measured at an indentation load of 98.1 N. Five indentations were made for each sample. The fracture toughness, K_{IC}, was obtained from the radial crack pattern of the indents and calculated using Shetty's equation[17]:

$$K_{IC} = 0.089\left(\frac{H_V P}{4L}\right)^{1/2} \quad (1)$$

where P is the load (98.1 N), H_V is the Vickers hardness and L is the length of the crack initiated at the edge of the indent.

3. Results and discussion

The densification behaviour through segments II–V (see Section 2) is shown in Fig. 1. A specimen with a relative density of 96% of the theoretical density of tetragonal zirconia was obtained after an SPS process of only 10 min under a compaction pressure of 100 MPa, with a dwell time of less than 1 min at a maximum temperature of 1100 °C. The piston position at the 450 °C dwell (start Segment II) is taken as a reference for the relative piston movement (ΔL). It can be seen in Fig. 1 that no significant densification is visible in segment II, in which the temperature increases from 450 °C to 850 °C and the pressure remains at 16 MPa. Upon increasing the pressure a large piston movement is achieved (segment III). In segment IV, when a pressure of 100 MPa has been achieved, the piston movement shows a linear dependence of temperature. During the dwell at

Table 1
Density of 8 mol% doped 3Y-TZP (3YZ-8C) nano-powder composites processed by spark-plasma sintering (SPS).

Code	Max. T (°C)	Dwell time (min)	ρ (%)
SPS-1	1000	5	76
SPS-2	1050	3	85
SPS-3	1100	1	96

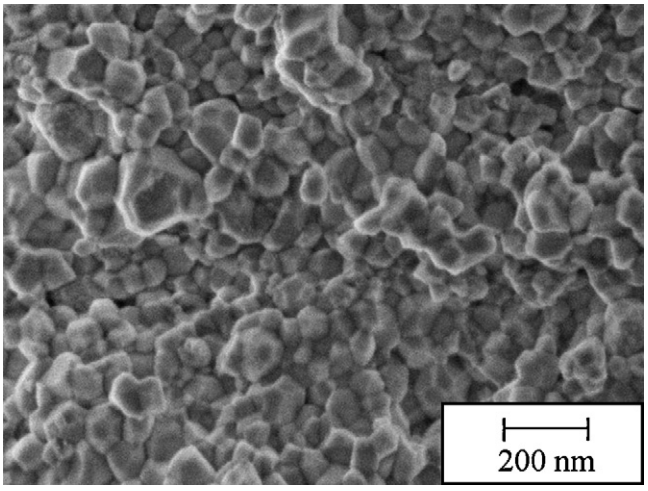

Fig. 2. SEM image of fractured surface of a sample after spark-plasma sintering.

1100 °C (segment V) the densification saturates quickly within 20 s. From this result, one can see that SPS is a very efficient technique for densifying 8 mol% CuO doped 3Y-TZP (3YZ-8C) nano-powder composites. In the case presented in this work, the specimen was fully densified within 4 min (assuming densification starts in segment III), while at least a few hours are needed in the case of pressureless sintering.[5,6]

Table 1 shows the final density of SPS specimens at different maximum temperature and dwell time. A decrease in maximum temperature of 50 °C results in a significant lower density (final density reduces to 85% and 76% in cases of SPS-2 and SPS-1, respectively). Longer dwell time does not effectively compensate the reduction in densification due to the lower temperature. Further results and discussion is focussed on samples of the SPS-3 type, as indicated in Table 1 and Fig. 1.

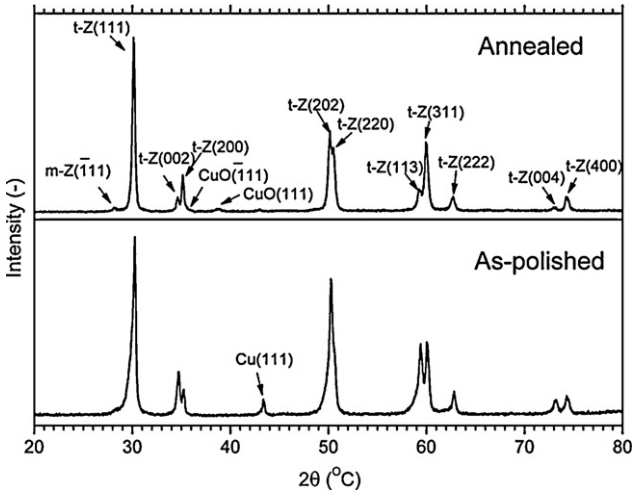

Fig. 4. XRD pattern of as-polished and 500 °C annealed samples (SPS). t-Z, m-Z, CuO and Cu denote tetragonal zirconia, monoclinic zirconia, Cu(II) oxide and metallic copper, respectively.

It is of interest to compare the microstructure of ceramic composites produced by SPS and PLS (pressureless sintering). The PLS results are described in detail in Ref.[6] An SEM image of a fractured surface and TEM images of an SPSed (spark-plasma sintered) sample are shown in Figs. 2 and 3, respectively. As can be seen from these figures the SPSed material exhibits a dense microstructure and an average grain size of about 70 nm. This value is significantly smaller than that of the composite prepared by PLS (120 nm and several micrometres for 960 °C and 1130 °C sintered samples, respectively).[6] It can be concluded that the SPS processing effectively suppresses grain growth during densification of the CuO doped 3Y-TZP nano-powder composite. This inhibition of grain growth is believed to be associated with the extremely fast heating rate and short sintering time in combination with a high external pressure.[8–11]

Fig. 4 shows the XRD pattern of polished 3YZ-8C samples after SPS and after subsequent annealing at 500 °C in air (no hold at this temperature). For the as-polished specimen the main phase can be identified as tetragonal zirconia (t-ZrO_2). It is important to point out that residual stresses are present in the as-polished specimen so that the XRD peaks are broadened and the intensity ratios between peaks are slightly different

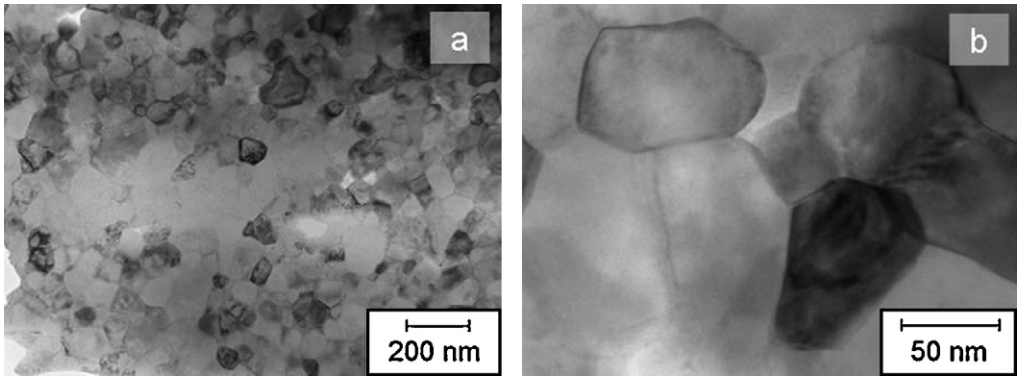

Fig. 3. TEM images of the as-spark-plasma sintered sample at different magnification.

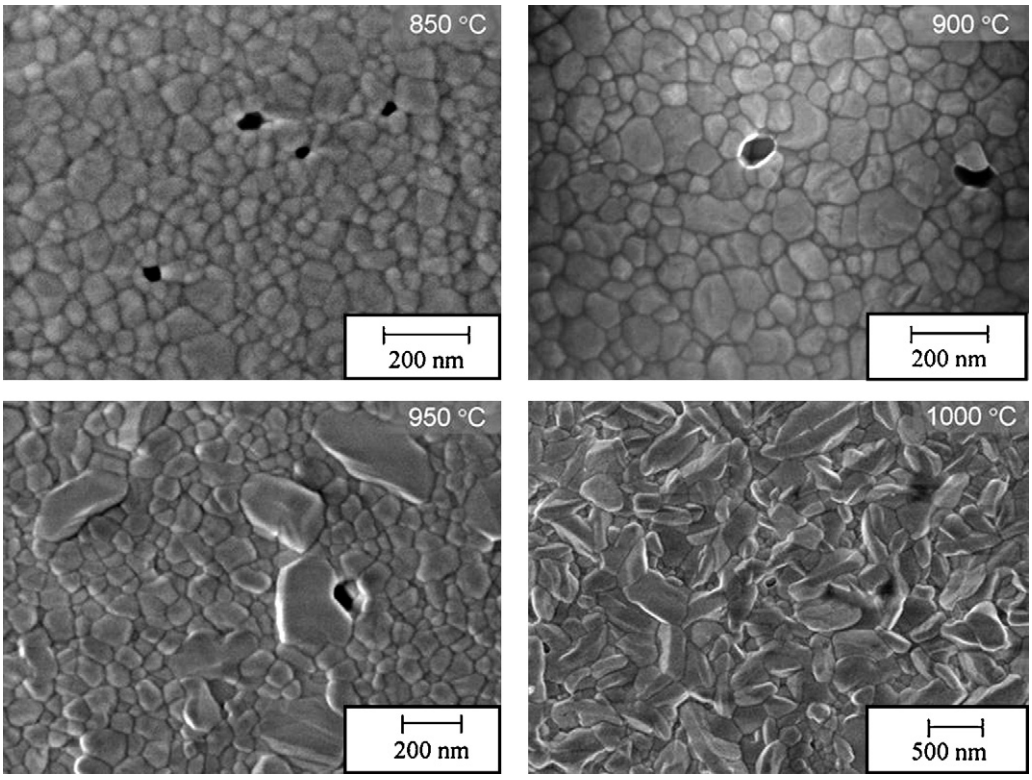

Fig. 5. SEM images of samples (SPS) annealed at various temperatures in an oxygen flow.

from standard references. After annealing at 500 °C in air the XRD signals get more narrow and the intensity ratio between the t-ZrO_2 signals are in good agreement with the value provided by the standard references. This change in pattern feature is attributed to the effective release of residual surface stresses in the specimen, which was introduced by cutting and polishing. At 2θ of about 28° a minor peak of monoclinic zirconia is observed after annealing. From this XRD pattern an amount of less than 3 vol.% monoclinic zirconia is estimated using Toraya's method.[15] This small amount of monoclinic zirconia is probably also present in the as-polished sample but is difficult to be observed because of peak broadening. Nevertheless, it can be stated that a sample densified by SPS contains almost only tetragonal zirconia. This result is very remarkable in contrast to the large amounts (80 vol.%) of monoclinic zirconia for ceramics prepared by pressureless sintering (PLS).[5–7]

A relative small signal is observed at 2θ of 43.5° in the XRD pattern of the as-polished SPSed specimen, which is ascribed to metallic Cu. After annealing at 500 °C the metallic Cu signal significantly reduces, while CuO ($\bar{1}$ 1 1) and CuO (1 1 1) reflections appear. These phenomena clearly indicate that the CuO phase in the starting 3YZ-8C powder is reduced to a metallic phase during the SPS process and re-oxidises by annealing in air. During the SPS processes a vacuum was applied to protect the graphite dies from oxidation, while additionally the powder was put in a graphite die/punch system with adjacent graphite sheets to facilitate sample removal. So a strong reducing environment was expected during the SPS process, in which Cu(II) could easily be reduced to Cu(0) at elevated temperatures. The presence of metallic Cu in these composites after SPS treatment was also visible by the metallic shine of the sample.

The significant difference in sintering behaviour and microstructure between the specimens produced by SPS and PLS can be explained by the influence of the processing method and processing temperatures on the reactions between CuO and 3Y-TZP, i.e., dissolution of CuO in the 3Y-TZP and formation of $Y_2Cu_2O_5$ in case of PLS[6] and the formation of Cu metal and tetragonal 3Y-TZP during SPS. In general it can be said that both reactions as observed during PLS are significantly suppressed by the extremely fast heating rate (400 °C min^{-1} from 450 °C to 850 °C and 100 °C min^{-1} from 850 °C to 1100 °C), or in other words the very short processing time (about 7 min in total) of the SPS process. It may be due to the fact that those reactions do not have sufficient time to occur to a sufficient extent. Consequently, densification in the 750–850 °C range is negligible (segment II in Fig. 1), whereas a significant densification as activated by CuO dissolution was observed in the corresponding temperature range in the case of PLS.[5,6] Additionally the destabilisation of tetragonal zirconia, arisen from the formation reaction of $Y_2Cu_2O_5$,[6] is prevented when the SPS procedure is applied. The reduction of CuO to metallic Cu, as revealed by XRD analysis (see Fig. 4), can also contribute to the retention of the tetragonal zirconia phase in the material densified by SPS. As described in Refs.,[6] the formation of $Y_2Cu_2O_5$ is a result of the reaction between CuO and yttria as segregated to the 3Y-TZP grain boundaries. Assuming metallic Cu does not react with Y_2O_3, the reduction of CuO obviously results in the removal of one reactant for this reaction and consequently prevents the for-

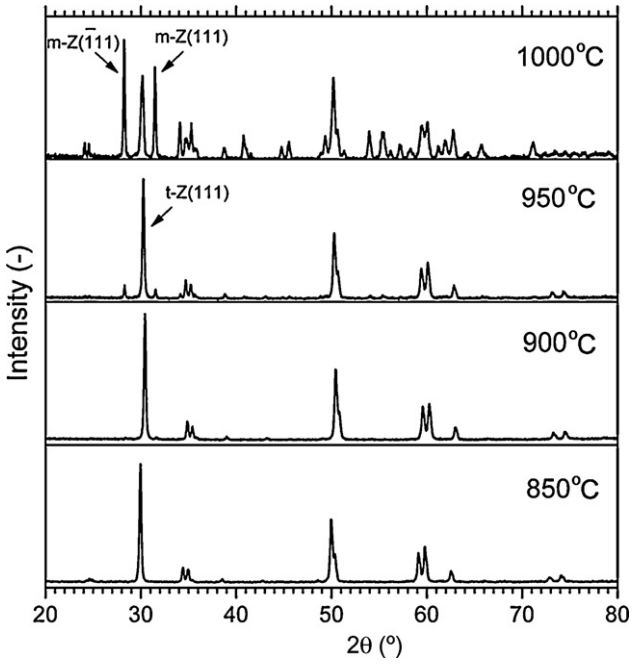

Fig. 6. XRD patterns of samples (SPS) annealed at various temperatures in an oxygen flow.

mation of $Y_2Cu_2O_5$. If this reaction takes place (as for PLS) it initiates the formation of the thermodynamic stable monoclinic zirconia phase (at $T < 1200\,^{\circ}C$) by reducing the kinetic energy barrier for phase transformation $(\Delta G^*)^{\circ}$.[6]

The microstructure of the SPS ceramic can be further adjusted by subsequent annealing. Fig. 5 shows SEM images of polished cross-sections of SPSed samples after annealing at various temperatures in an oxygen flow. The XRD patterns of these annealed specimens are shown in Fig. 6. The volume fraction of monoclinic zirconia phase in these specimens is listed in Table 2 and compared with 3YZ-8C produced by PLS.[6]

After annealing at 850 °C the specimen shows identical grain size and zirconia crystal phase as the as-SPSed specimen (i.e., an average grain size of 70 nm and almost pure tetragonal zirconia). For a sample, annealed at 900 °C for 1 h, only a slight increase in average grain size (110 nm) can be observed. In contrast to the almost negligible microstructure development during annealing ≤900 °C, some remarkable changes in microstructure are observed after annealing ≥950 °C. The sample annealed at 950 °C shows a non-uniform grain size distribution. A significant amount of large grains with a size of more than 200 nm and an elongated shape are visible in the cross-section image (Fig. 5; 950 °C). However the average size of the grains surrounding these large ones is only 120 nm. This result implies that a strong grain growth starts. It is also revealed by XRD analysis that around 30 vol.% of monoclinic zirconia phase was formed during annealing at 950 °C (Fig. 6 and Table 2). After annealing at 1000 °C for 1 h almost all grains became elongated. The length of these grains is as large as 500 nm. Accompanying with this drastic microstructure evolution, 75 vol.% of monoclinic zirconia phase was formed.

Table 2
Properties of 3YZ-8C ceramics produced by different techniques.

Code[a]	ρ (%)	V_m (vol.%)	d	H_V (GPa)	K_{IC} (MPa m$^{1/2}$)
PS1130	95	80	>1 μm	8.7 ± 0.2	3.7 ± 0.1
PS960	96	80	120 nm	10.9 ± 0.2	3.7 ± 0.1
SA-	96	0	70 nm	n.m.	n.m.
SA850	96	0	70 nm	11.4 ± 0.9	4.3 ± 0.4
SA900	96	0	110 nm	11.8 ± 0.2	5.4 ± 0.7
SA950	96	30	120 nm	10.5 ± 0.5	3.1 ± 0.3
SA1000	96	75	~500 nm	9.3 ± 0.1	3.8 ± 0.1

ρ: relative density; V_m: volume fraction of m-ZrO_2; d: average grain size; H_V: Vickers hardness; K_{IC}: fracture toughness. n.m.: not measured (values expected to be identical with SA850).

[a] PSx: pressureless sintered at x °C; SAx: spark-plasma sintered (SPS-3) and annealed at x °C for 1 h (SA: as-spark-plasma sintered—not-annealed).

The significant microstructure change during annealing above 950 °C can also be explained by the reactions between CuO and 3Y-TZP grains, which are effectively suppressed during the SPS process. During this 950 °C annealing treatment the Cu phase has re-oxidised and reactions between 3Y-TZP and CuO can occur, i.e., CuO dissolution in the 3Y-TZP grain boundaries and the formation reaction of $Y_2Cu_2O_5$. The consequences of these reactions during annealing are the strong grain growth and tetragonal to monoclinic zirconia phase transformation.[6]

Combining techniques like pressureless sintering, SPS and subsequent annealing, one has extended tools to manipulate the microstructure of these CuO doped 3Y-TZP composite ceramics, and, moreover, to adjust properties of the material. As an example of adjusting properties by means of microstructure manipulating, hardness and fracture toughness of the 3TZ-8C ceramics are presented in Table 2. All these 3TZ-8C ceramics possess a relative density of more than 95% (presence of monoclinic zirconia phase is taken into account for theoretical density calculation). The dependence of hardness (H_V) on grain size is clearly revealed for the 3TZ-8C ceramic composites. The materials with small grain sizes exhibit remarkable higher hardness values ($H_V \geq 10.5$ GPa when $d < 200$ nm) than the coarse-grained materials ($H_V \leq 9.5$ GPa when $d > 500$ nm). On the other hand, fracture toughness (K_{IC}) shows a remarkably dependence on the combination of the monoclinic zirconia content and grain size. All materials containing 75–80 vol.% of monoclinic zirconia show similar fracture toughness ($K_{IC} \approx 3.7$ MPa m$^{1/2}$). The SPSed material annealed at 850 °C, which possessed no monoclinic zirconia phase and an average grain size of 70 nm, gives a slightly higher fracture toughness ($K_{IC} \approx 4.3$ MPa m$^{1/2}$). If the tetragonal zirconia phase is maintained and a slight increase in grain size is achieved, i.e., after annealing at 900 °C for 1 h, an improvement in fracture toughness ($K_{IC} \approx 5.4$ MPa m$^{1/2}$) is observed. However, generating 30 vol.% monoclinic zirconia in the material by annealing at 950 °C significantly decreases the fracture toughness ($K_{IC} \approx 3.1$ MPa m$^{1/2}$). It is concluded that SPS processing followed by annealing at 900 °C for 1 h is the optimal fabrication procedure for 3TZ-8C nano-ceramics from a mechanical point of view.

For a profound understanding of the microstructural influence on mechanical properties of the 3TZ-8C ceramics, more research is of course required. Nevertheless, the results as presented here have clearly shown that microstructure and properties of these

ceramics can be adjusted to a significant extent by utilising various processing techniques.

It is important to note that the microstructure normally matters for many properties of a ceramic material. In this sense some other structural and functional properties of the CuO doped 3Y-TZP composite ceramic, e.g. (super)plastic, tribological and electrical properties can be tuned by utilising different processing techniques. Tuning mechanical properties of the composite ceramic is shown here just as an example. More investigation on tuning other properties of CuO doped 3Y-TZP composite ceramic (and other materials) by manipulation of microstructure, via control of processing, is of great interest.

4. Conclusions

In summary we have proven that spark-plasma sintering (SPS) is a very efficient technique for producing a dense nanostructured CuO doped 3Y-TZP ceramic (average grain size: 70 nm). The SPS composite possesses a phase composition of purely tetragonal zirconia with metallic Cu, whereas, 80 vol.% of monoclinic zirconia phase is always present in the conventionally (pressureless) sintered composite. This difference in microstructure is caused by the extremely fast heating rate as well as the strongly reducing atmosphere associated with SPS processing. As one of the consequences, the tetragonal to monoclinic zirconia phase transformation caused by formation of $Y_2Cu_2O_5$ as observed in the case of conventional sintering is totally prevented.

Moreover, the microstructural properties, i.e., grain size and crystal structure of the zirconia phase in CuO doped 3Y-TZP nano-powder composites can be manipulated to a large extent by utilising different processing techniques, including pressureless sintering, spark-plasma sintering and subsequent annealing. Hardness and fracture toughness of dense nano-ceramics of 8 mol% CuO doped 3Y-TZP can be tuned by using different processing techniques and is presented as an example for adjusting material properties via microstructural manipulation.

References

1. Mayo, M. J., Seidensticker, J. R., Hauge, D. C. and Carim, A. H., Surface chemistry effects on the processing and superplastic properties of nanocrystalline oxide ceramics. *Nanostruct. Mater.*, 1999, **11**(2), 271–282.
2. Hwang, C. M. J. and Chen, I.-W., Effect of a liquid phase on superplasticity of 2-mol%-Y_2O_3-stabilized tetragonal zirconia polycrystals. *J. Am. Ceram. Soc.*, 1990, **73**(6), 1626–1632.
3. Ran, S., Winnubst, L., Blank, D. H. A., Pasaribu, H. R., Sloetjes, J.-W. and Schipper, D. J., Effect of microstructure on the tribological and mechanical properties of CuO-doped 3Y-TZP ceramics. *J. Am. Ceram. Soc.*, 2007, **90**(9), 2747–2752.
4. Pasaribu, H. R., Sloetjes, J. W. and Schipper, D. J., Friction reduction by adding copper oxide into alumina and zirconia ceramics. *Wear*, 2003, **255**(1–6), 699–707.
5. Ran, S., Winnubst, A. J. A., Koster, H., de Veen, P. J. and Blank, D. H. A., Sintering behaviour and microstructure of 3Y-TZP + 8 mol% CuO nano-powder composite. *J. Eur. Ceram. Soc.*, 2007, **27**(2–3), 683–687.
6. Winnubst, L., Ran, S., Speets, E. A. and Blank, D. H. A., Analysis of reactions during sintering of CuO-doped 3Y-TZP nano-powder composites. *J. Eur. Ceram. Soc.*, 2009, **29**(12), 2549–2557.
7. Ran, S., Winnubst, A. J. A., Wiratha, W. and Blank, D. H. A., Sintering behavior of 0.8 mol%-CuO-doped 3Y-TZP ceramics. *J. Am. Ceram. Soc.*, 2006, **89**(1), 151–155.
8. Groza, J. R. and Zavaliangos, A., Sintering activation by external electrical field. *Mater. Sci. Eng.*, 2000, **A287**, 171–177.
9. Vanmeensel, K., Laptev, A., Hennicke, J., Vleugels, J. and Van der Biest, O., Modelling of the temperature distribution during field assisted sintering. *Acta Mater.*, 2005, **53**, 4379–4388.
10. Shen, Z. and Nygren, M., Microstructural prototyping of ceramics by kinetic engineering: application of spark plasma sintering. *Chem. Rec.*, 2005, **5**, 173–184.
11. Shen, Z., Zhao, Z., Peng, H. and Nygren, M., Formation of tough interlocking microstructures in silicon nitride ceramics by dynamic ripening. *Nature*, 2002, **417**, 266–269.
12. Khor, K. A., Cheng, K. H., Yu, L. G. and Boey, F., Thermal conductivity and dielectric constant of spark plasma sintered aluminium nitride. *Mater. Sci. Eng.*, 2003, **A347**, 300–305.
13. Su, X., Wang, P., Chen, W., Shen, Z., Nygren, M., Yibing, C. *et al.*, Effects of composition and thermal treatment on infrared transmission of Dy-a-sialon. *J. Eur. Ceram. Soc.*, 2004, **24**, 2869–2877.
14. Winnubst, L., Veen, P.J. de, Ran, S. and Blank, D.H.A., Synthesis and characteristics of nanocrystalline 3Y-TZP and CuO powders for ceramic composites. Ceramics Int., 2010, in press; DOI: 10.1016/j.ceramint.2009.08.001.
15. Toraya, H., Yoshimura, M. and Somiya, S., Calibration curve for quantitative analysis of the monoclinic-tetragonal ZrO_2 system by X-ray diffraction. *J. Am. Ceram. Soc.*, 1984, **67**(6), C119–C121.
16. Mendelson, M. I., Average grain size in polycrystalline ceramics. *J. Am. Ceram. Soc.*, 1969, **52**, 443–446.
17. Shetty, D. K., Wright, I. G., Mincer, P. N. and Clauer, P. N., Indentation fracture of WC-Co cermets. *J. Mater. Sci.*, 1985, **20**, 1873–1882.